MEASUREMENT OF THE CHARM STRUCTURE FUNCTION OF THE PHOTON AT LEP*

Á. CSILLING
CERN, CH-1211, Geneva, Switzerland†
E-mail: Akos.Csilling@cern.ch

Charm production is studied in deep-inelastic electron-photon scattering using OPAL data at e^+e^- centre-of-mass energies from 183 to 209 GeV. Charm quarks are identified by exclusive reconstruction of $D^\star$ mesons. The cross-section of $D^\star$ production is measured in a restricted kinematic region, and then extrapolated to the total charm production cross-section and the charm structure function of the photon. For $x > 0.1$ the measurement is well described by Monte Carlo models and perturbative QCD calculations but for $x < 0.1$ the predictions are lower than the data both in the directly measured region and after the extrapolation.

1 Introduction

The charm component of the photon structure function, $F_{2,c}^{\gamma}$, has been measured by OPAL at LEP2 by applying the well established method of exclusive $D^\star$ reconstruction to deep-inelastic electron-photon scattering events. The determination of $F_{2,c}^{\gamma}$ exploits the fact that the differential cross-section as function of Q^2 and Bjorken x is proportional to $F_{2,c}^{\gamma}(x, Q^2)$. [1]

Due to the large scale established by their masses, the contribution to F_2^{γ} from charm quarks can be calculated in perturbative QCD, and predictions have been evaluated [2] at next-to-leading order (NLO) accuracy. $F_{2,c}^{\gamma}$ receives contributions from the point-like and hadron-like components of the photon structure, with the hadron-like component dominating at very low values of x and the point-like part accounting for most of $F_{2,c}^{\gamma}$ for $x > 0.1$.

The preliminary results presented here [3] extend the earlier measurement [4] of $F_{2,c}^{\gamma}$ using basically the same analysis strategy. It is based on 654.1 pb^{-1} of data for e^+e^- centre-of-mass energies from 183 to 209 GeV, recorded by the OPAL experiment in the years 1997–2000.

*Presented at the International Conference on the Structure and Interactions of the Photon, including the 14th International Workshop on Photon-Photon Collisions, Ascona, Switzerland, 2-7 September, 2001.

†On leave of absence from KFKI Research Institute for Particle and Nuclear Physics, H-1525 Budapest, P.O.Box 49, Hungary

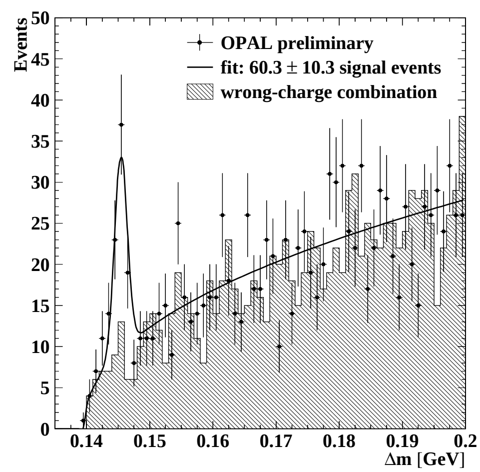

Figure 1. Distribution of the difference between the D* and D^0 candidate masses. The data are shown as points with statistical errors, while the histogram represents the combinatorial background estimated using events with wrong-charge combinations for the decay products of the D* mesons. The curve is the result of the fit to the data.

2 Data selection

The most important cuts used in the selection of deep-inelastic electron-photon scattering events containing a D* are summarised below.

1. An electron candidate must be present with an energy $E_{\rm tag} > 0.5E_{\rm b}$ and a polar angle in the ranges $33 < \theta_{\rm tag} < 55$ mrad (SW) or $60 < \theta_{\rm tag} <$ 120 mrad (FD), corresponding to $5 < Q^2 < 100$ GeV^2.
2. Double-tag events are eliminated by requiring that the sum of all energies in the SW and FD detectors opposite to the tag are below $0.25E_{\rm b}$
3. An exclusively reconstructed D* candidate must be present with a transverse momentum $p_{\rm T}^{\rm D^\star} > 1(3)$ GeV for SW(FD)-tagged events and a pseudorapidity $|\eta^{\rm D^\star}| < 1.5$. The D* meson must decay into D$^0\pi$ with the D^0 decaying into the charged particles Kπ or K$\pi\pi\pi$.

Figure 1 shows the difference between the D* and D^0 candidate masses for both decay channels combined. A clear peak is observed around 0.145 GeV, the mass difference between the D* and the D^0 mesons. An unbinned maximum likelihood fit to this distribution gives 60.3 ± 10.3 signal events above the combinatorial background from deep-inelastic electron-photon scattering events $\rm e^+e^- \to e^+e^- q\bar{q}$ with q=uds. The expected background from all other

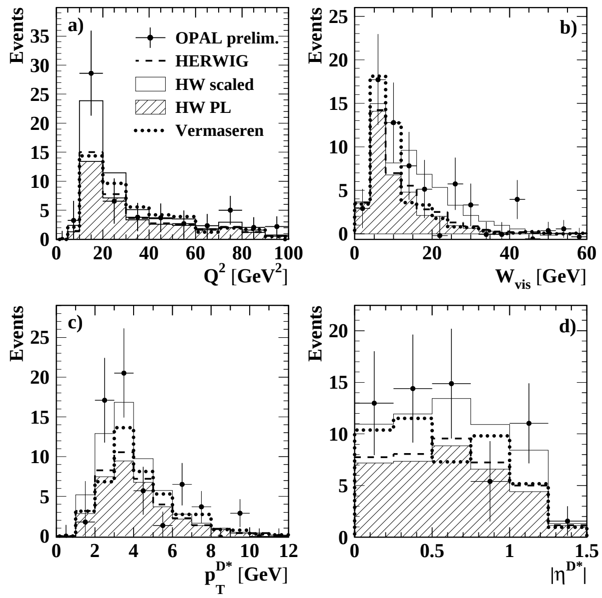

Figure 2. Data distributions compared to the HERWIG and Vermaseren predictions. For HERWIG several predictions are shown: the full prediction, the point-like component alone (HW PL), and a superposition of the HERWIG point-like prediction together with a scaled hadron-like prediction, denoted by HW scaled.

processes that potentially contain $D^\star$ mesons in the final state is found to be negligible using Monte Carlo simulations.

Figure 2 shows the distributions of two global event quantities, Q^2 and $W_{\rm vis}$, and two variables related to the kinematics of the $D^\star$ candidates, $p_T^{D^\star}$ and $|\eta^{D^\star}|$. The data are compared to the absolute predictions of the HERWIG6.1 [5] and Vermaseren [6] leading order Monte Carlo programs.

To get a better description of the data, the hadron-like component of the HERWIG prediction has been fitted to the $x_T^{D^\star} = 2p_T^{D^\star}/W_{\rm vis}$ distribution shown in Figure 3 while keeping the point-like part fixed, resulting in a scale factor of 6.6 ± 2.7. There are several possible sources for this difference. The NLO prediction itself has a significant uncertainty due to variations of the charm quark mass and the renormalisation and factorisation scales, the gluon distribution of the photon has large experimental errors, and uncertainties in the shape and the modelling of the $p_T^{D^\star}$ distribution can change the efficiency for the selected events.

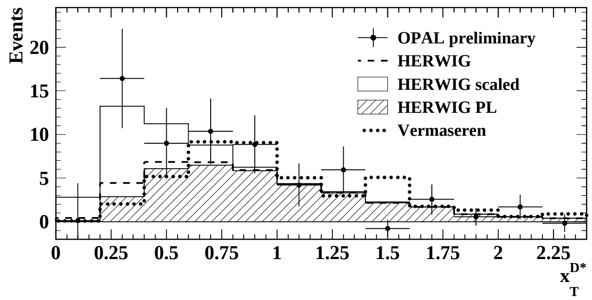

Figure 3. The measured $x_{\mathrm{T}}^{\mathrm{D}^\star}$ distribution compared to the predictions described in the caption of Figure 2.

This scaled HERWIG prediction, also shown in Figure 2, is used to estimate the signal selection efficiency. The difference between the results obtained with the scaled and the original HERWIG models is taken into account as a systematic uncertainty.

3 Results

Table 1 summarises the cross-section of $\mathrm{D}^\star$ production in deep-inelastic electron-photon scattering measured in the kinematic region defined by the event selection. The total cross-section for $\mathrm{c\bar{c}}$ production in deep-inelastic electron-photon scattering, shown in Figure 4a), is the result of an extrapolation to the whole kinematic region using the HERWIG scaled model. The value of the charm structure function of the photon, $F_{2,\mathrm{c}}^{\gamma}(x,\langle Q^2\rangle)/\alpha_{\mathrm{em}}$, averaged over the corresponding bin in x, shown in Figure 4b), is obtained using the ratio $F_{2,\mathrm{c}}^{\gamma}(x,\langle Q^2\rangle)/\alpha_{\mathrm{em}}/\sigma(\mathrm{e^+e^-} \rightarrow \mathrm{e^+e^-\,c\bar{c}}\,X)$ given by the NLO calculation. [2]

Table 1. The cross-section $\sigma^{\mathrm{D}^\star}$ measured in the restricted region, compared to Monte Carlo predictions. The numbers in parentheses refer to the point-like and hadron like components.

	$0.0014 < x < 0.1$	$0.1 < x < 0.87$
OPAL	$4.7 \pm 1.3 \pm 0.9$	$3.0 \pm 0.9 \pm 0.4$
HERWIG	1.02 (0.65 + 0.37)	2.05 (2.02 + 0.03)
HW scaled	3.10 (0.65 + 2.45)	2.23 (2.02 + 0.21)
Vermaseren	0.84	2.81

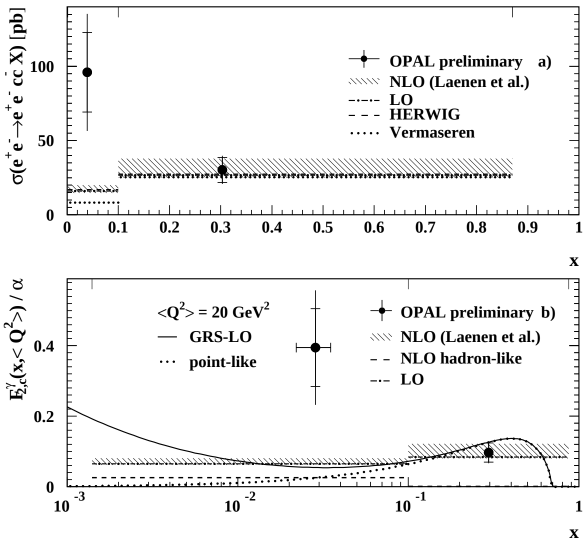

Figure 4. Preliminary OPAL results for a) $\sigma(\mathrm{e}^+\mathrm{e}^- \to \mathrm{e}^+\mathrm{e}^-\,\mathrm{c\bar{c}}\,X)$, with $5 < Q^2 < 100\ \mathrm{GeV}^2$ and b) $F^{\gamma}_{2,\mathrm{c}}(x, \langle Q^2 \rangle)/\alpha_{\mathrm{em}}$. The band for the NLO calculation [2] indicates the theoretical uncertainties.

All models and predictions shown in Figure 4 are in good agreement with the measurement for $x > 0.1$, where the purely perturbative point-like process is dominant and both the experimental and the theoretical uncertainties are moderate.

On the other hand, for $x < 0.1$ the measurement lies more than two standard deviations above the predictions, which contain an approximately equal contribution from the point-like and hadron-like processes. This difference is also observed in the comparisons to the Monte Carlo models in the directly measured kinematic region, where the extrapolation uncertainties are avoided. Unfortunately, no theoretical calculations are available for comparison in the restricted phase-space.

References

1. R. Nisius, Phys. Rep. **332**, 165–317 (2000).
2. E. Laenen et al., Phys. Rev. **D49**, 5753–5768 (1994); E. Laenen and S. Riemersma, Phys. Lett. **B376**, 169–176 (1996).
3. OPAL Collaboration, G. Abbiendi et al., OPAL PN490.

4. OPAL Collaboration, G. Abbiendi et al., Eur. Phys. J. **C16**, 579–596 (2000).
5. G. Marchesini et al., Comp. Phys. Comm. **67**, 465–508 (1992).
6. J.A.M. Vermaseren, J. Smith, and G. Grammer Jr., Phys. Rev. **D19**, 137–143 (1979); J.A.M. Vermaseren, Nucl. Phys. **B229**, 347–371 (1983).